THE JOURNAL OF BIOLOGICAL CHEMISTRY VOL. 286, NO. 25, pp. 22275–22282, June 24, 2011

Haploid Insufficiency of Suppressor Enhancer Lin12 1-like (SEL1L) Protein Predisposes Mice to High Fat Diet-induced Hyperglycemia*[S]

Received for publication, March 11, 2011, and in revised form, April 22, 2011 Published, JBC Papers in Press, May 2, 2011, DOI 10.1074/jbc.M111.239418

Adam B. Francisco[1], **Rajni Singh**[1], **Haibo Sha, Xi Yan, Ling Qi, Xingen Lei, and Qiaoming Long**[2]

From the Department of Animal Science, College of Agriculture and Life Sciences, Cornell University, Ithaca, New York 14850

Increasing evidence suggests that endoplasmic reticulum (ER) stress plays an important role in the pathogenesis of type 2 diabetes mellitus. SEL1L is an ER membrane protein that is highly expressed in the pancreatic islet and acinar cells. We have recently reported that a deficiency of SEL1L causes systemic ER stress and leads to embryonic lethality in mice. Here we show that mice with one functional allele of *Sel1l* (*Sel1l*$^{+/-}$) are more susceptible to high fat diet (HFD)-induced hyperglycemia. *Sel1l*$^{+/-}$ mice have a markedly reduced β-cell mass as a result of decreased β-cell proliferation. Consequently, *Sel1l*$^{+/-}$ mice are severely glucose-intolerant and exhibit significantly retarded glucose-stimulated insulin secretion. Pancreatic islets from *Sel1l*$^{+/-}$ mice stimulated with a high concentration of glucose *in vitro* express significantly higher levels of unfolded protein response genes than those from wild-type control mice. Furthermore, dominant-negative interference of SEL1L function in insulinoma cell lines severely impairs, whereas overexpression of SEL1L efficiently improves protein secretion. Taken together, our results indicate that haploid insufficiency of SEL1L predispose mice to high fat diet-induced hyperglycemia. Our findings highlight a critical and previously unknown function for SEL1L in regulating adult β-cell function and growth.

Type 2 diabetes mellitus (T2DM)[3] is a major chronic disease currently affecting over 24 million Americans with annual costs exceeding $170 billion (1). Deficit in β-cell mass and intra-islet amyloid deposition are hallmark features of the islet in T2DM (2). Obesity is a well characterized risk factor for the development of T2DM (3, 4). The molecular mechanisms underlying the β-cell failure in T2DM and by which obesity promotes β-cell failure and intracellular amyloidogenesis remain elusive.

Accumulating evidence suggests that stress in the endoplasmic reticulum (ER) plays an important causal role in the pathogenesis of T2DM (5, 6). The ER is a specialized organelle where nearly all secreted and membrane proteins undergo post-translational modifications such as glycosylation, disulfide bond formation, folding, and multimeric protein complex assembling (7, 8). Properly folded/assembled proteins travel through the secretory pathway and reach various cellular destinations, whereas nonnative or unassembled proteins are retained in the ER lumen and eventually retrotranslocated into the cytosol for degradation by the proteasomal system (9). Disequilibrium of ER protein load and folding capacity results in accumulation of unfolded/misfolded proteins in the ER lumen, leading to ER stress (10). In response to ER stress, cells activate at least three intracellular signal transduction pathways, cumulatively referred to as the unfolded protein response (11). The unfolded protein response, coordinated by three distinct ER stress signal transducers, PERK, IRE1a, and ATF6 (12), result in a general attenuation of protein translation (13) and an increased expression of ER chaperones and ER-associated degradation machinery (9, 14). Consequently, there is a reduced production of proteins that enter the ER, and there is an increase in the capacity of the ER to handle unfolded proteins. Together, these adaptive measures provide a multifaceted mechanism to maintain ER homeostasis under temporary and reversible ER stress conditions.

ER homeostasis is particularly important for the function and viability of professional secretory cells such as the pancreatic β-cell (15, 16). The unique function of the β-cell is to integrate nutrient signals into an appropriate insulin secretory rate to maintain normal glucose homeostasis. In response to serum glucose stimulus, β-cells secrete insulin from a readily available pool while activating proinsulin biosynthesis in the ER (17). Proinsulin undergoes protein folding and disulfide bond formation in the lumen of the ER (17). Properly folded proinsulin is then released to the Golgi apparatus and packaged into secretory granules, where conversion of proinsulin into mature insulin takes place (18). Because of the rapid fluctuation of serum glucose levels in animals, it is essential that β-cells control proinsulin folding in the ER with exquisite sensitivity (19). It has been suggested that conditions either evoking an overload of newly synthesized proinsulin or compromising protein folding capacity in the ER may negatively affect the homeostasis of β-cells, leading to ER stress and onset of T2DM (6). Consistent with this, markers of ER stress have been shown to be up-regulated in the islets from T2DM patients (20, 21) and from several animal models of obesity and diabetes (22–25).

* This work was supported by the College of Agriculture and Life Sciences and the Vertebrate Functional Genomics Center, Cornell University (to Q. L.).

[S] The on-line version of this article (available at http://www.jbc.org) contains supplemental Figs. S1–S3.

[1] Both authors contributed equally to this work.

[2] To whom correspondence should be addressed: Dept. of Animal Science, 321 Morrison Hall, Cornell University, Tower Rd., Ithaca, NY 14850. Tel.: 607-254-5380; Fax: 607-255-9829; E-mail: ql39@cornell.edu.

[3] The abbreviations used are: T2DM, type 2 diabetes mellitus; ER, endoplasmic reticulum; HFD, high fat diet; *Sel1l*, suppressor enhancer Lin12 1-like; GSIS, glucose-stimulated insulin secretion; rtTA, reverse tet transactivator; 4-PBA, phenylbutyric acid; NC, normal chow; UPR, unfolded protein response.

Suppressor enhancer lin12 1-like (*Sel1l*) is highly expressed in the developing and matured pancreatic cells (26, 27). *Sel1l* encodes an ER membrane protein (type I) with a complex domain structure (28). Previous biochemical and molecular studies *in vitro* showed that SEL1L nucleates an ER membrane protein complex that is required for dislocation of unfolded or misfolded proteins from the ER lumen into the cytosol for degradation (29–34). We recently reported that mice homozygous for a gene trap mutation in *Sel1l* develop systemic ER stress and die during mid-gestation (35). In addition, we revealed that SEL1L deficiency impairs the growth and differentiation of pancreatic epithelial cells during early mouse embryonic development (36). These genetic data are consistent with the hypothesis that SEL1L regulates ER homeostasis in mammalian cells by facilitating ER-associated degradation of unfolded proteins (32, 33).

The physiological role of SEL1L in adult islets remains unclear. Here, we show that mice heterozygous for the gene-trap mutation in *Sel1l* (*Sel1l*$^{+/-}$) are more susceptible to diet-induced hyperglycemia. *Sel1l*$^{+/-}$ mice are glucose intolerant and have a reduced β-cell mass. Cultured islets from *Sel1l*$^{+/-}$ mice show significantly higher expression of unfolded protein response marker genes than wild-type control islets. Thus, our data suggest that SEL1L is a critical regulator of β-cell function and growth in adult mice.

MATERIALS AND METHODS

Mice—Generation of *Sel1l* gene trap mice (*Sel1l*$^{+/-}$) was described previously (35). For physiological studies, *Sel1l*$^{+/-}$ mice were back-crossed to C57/B6 mice for five generations and then intercrossed to generate wild-type and *Sel1l*$^{+/-}$ mice. All mice were weaned at 3 weeks of age, and genotyping was done by PCR using the following primers: F1-Sel1l, 5′-TGGGACAGAGCGGGCTTGGAAT-3′; R1-Sel1l, 5′-CACCAGGAGTCAAAGGCATCACTG-3′; R-βGeo, 5′-ATTCAGGCTGCGCAACTGTTGGG-3′.

For high fat diet feeding experiments, wild-type and heterozygous male mice at 6–8 weeks of age were put on a TD.06414 diet (Harlan, Madison, WI), which contains 23.5, 27.3, and 34.3% protein, carbohydrate, and fat, respectively. All animal experiments were performed in accordance with the Cornell Animal Care and Use Guidelines.

Physiological Studies—Fasting blood glucose was measured using an Ascensia Elite XL glucometer (Bayer). Glucose and insulin tolerance tests and glucose-stimulated insulin secretion (GSIS) were performed essentially as described (37). For the glucose tolerance test, mice were fasted for 6–8 hours and then injected intraperitoneal with 2 g of D-glucose/kg body weight. Blood glucose was measured at 0, 5, 15, 30, 60, and 120 min after glucose injection. For the insulin tolerance test, mice were fasted for 6 hours and then injected intraperitoneally with 1.0 unit of regular human insulin (Eli Lilly, Indianapolis, IN)/kg body weight dissolved in phosphate-buffered saline (PBS). Blood glucose was measured at 0, 5, 15, 30, 60, and 120 min post-insulin injection. 4-Phenylbutyric acid (4-PBA) was administered into mice by gavage as previously described (38).

Morphological Analysis of Pancreas—Pancreata were fixed in 4% paraformaldehyde overnight at 4 °C and paraffin embedded. Pancreatic sections were cut at 5-μm and mounted on glass slides. Insulin immunostaining was performed by using guinea pig anti-human insulin (Linco, 1:1000). Secondary antibodies used were either Cy2- or HRP-conjugated donkey anti-guinea pig immunoglobulin (IgG) (Jackson ImmunoResearch Laboratories, 1:500). Nuclear counterstaining was performed using 4′,6-diamidino-2-phenylindole (DAPI). β-Cell mass was determined as previously described (37). Briefly, total pancreatic and β-cell areas were measured using the AxioVision software (Version 4.1). β-Cell mass was calculated by multiplying the total pancreatic weight with the percentage of β-cell area. To determine β-cell proliferation, pancreatic sections were co-immunostained with a mouse monoclonal anti-Ki67 (Vector Laboratories, 1:500) and anti-insulin antibodies. Nuclei were counterstained with DAPI. The percentage of Ki67$^+$ cells was derived by dividing the total number of counted β-cell nuclei with the number of Ki67$^+$ nuclei. β-Cell apoptosis was assessed by TUNEL assay using the ApopTag *In Situ* Apoptosis detection kit (Chemicon, Temecula, CA) according to the manufacturer's instructions. All images were acquired using an Axiovert 40 microscope (Zeiss) equipped with an AxioCam camera.

Pancreatic Insulin Content—Pancreatic insulin content was determined as previously described (39). Briefly, pancreata were removed from mice and homogenized in 1 ml of acid ethanol (95% ethanol, 10.2 N HCl in a 50:1 ratio). The homogenized pancreata were incubated overnight at 4 °C and centrifuged. Insulin concentration in the supernatant was determined using ELISA (Crystal Chem, Downers Grove, IL) and normalized by total protein content.

Islet Isolation and in Vitro GSIS—Mouse islet isolation was performed as previously described (40). Briefly, after sacrifice of each mouse, the pancreas was perfused with 1× Hanks' balanced salt solution, pH 7.4, containing 2.0 mg/ml type V collagenase (Sigma). The inflated pancreas was removed from the body and incubated at 37 °C for 20 min. The collagenase-digested pancreas was vigorously shaken for 5 s, washed 3 times with 5–7 ml of ice-cold 1× Hanks' balanced salt solution buffer, and re-suspended in 2 ml of 28% Ficoll (VWR, West Chester, PA). The islet and acinar mixture was loaded onto the top of gradient Ficoll solutions and centrifuged at 2250 rpm for 7 min at 4 °C. Islets were collected and washed three times with ice-cold 1× Hanks' balanced salt solution before processing for further analysis.

GSIS for islets was performed as previously described with minor modifications (41). Briefly, isolated islets were washed twice with 1× KRBH buffer (118.5 mM NaCl, 2.54 mM $CaCl_2 \cdot 2H_2O$, 1.19 mM KH_2PO_4, 4.74 mM KCl, 25 mM $NaHCO_3$, 1.19 mM $MgSO_4 \cdot 7H_2O$, 10 mM HEPES, 0.1% BSA, 5 mM glutamic acid, 5 mM fumaric acid, 5 mM pyruvic acid, pH 7.4) and equilibrated in the same buffer containing 2.8 mM glucose for 60 min at 37 °C. Islets were then incubated in 1× KRBH buffer containing either 2.8 or 16.8 mM glucose for 30 min at 37 °C. The low and high glucose-incubated islets were briefly centrifuged, and the supernatants were assayed for secreted insulin, which was normalized to islet insulin content. Islet insulin content was normalized to the total protein concentration.

RNA Extraction and Quantitative RT-PCR—RNA isolation and real-time RT-PCR were performed as previously described

(35). PCR primers were designed using the PrimerSelect program of Lasergene 7.1 Sequence Analysis Software (DNAStar, Madison, WI). Relative mRNA expression was calculated by dividing the expression value in *Sel1l*$^{+/-}$ islets (set to 1) with that in wild-type islets.

Cell Culture—Min6 cells were maintained as previously described (42). For establishing stable cell lines, Min6 cells were grown to 50–60% confluency, trypsinized, washed three times in cold PBS, and resuspended in PBS. 5.6×10^6/ml was mixed with 10–20 μg of plasmid DNA, electroporated (0.24 kV and 500 microfarads) and plated into a 24-well plate. The electroporated Min6 cells were incubated in regular media for 48 h and then in neomycin resistance selection medium (G418 at 1 mg/ml) for 10 days. Stable Min6 clones were maintained in regular medium. GSIS for Min6 cells was performed essentially as previously described (43).

INS-1 cells were maintained as previously described (44). For generation of stable cell lines, INS-1 cells were seeded at a confluency of <10% and infected overnight with lentivirus expressing the reverse tet transactivator (rtTA), rtTA plus SEL1L-GFP, or rtTA plus dSEL1L-GFP. To induced expression of transgenes, doxycycline (Sigma) was added into the culture medium of Min6 and INS-1 cells (200 μg/ml).

Transient transfection and *Gaussia* luciferase (G-luc) assay in Min6 cells were performed as previously described (35). Cell growth profile was generated, and thymidine incorporation assay was performed as previously described (45).

Western Blot Analysis—Preparation of tissue/cell lysates, protein quantification, electrophoresis, and blotting were performed as previously described (35). Immunodetection was carried out using the Western blotting Luminol Reagent kit (Origene) according to the manufacturer's specifications. The primary antibodies used were: GFP (Abcam, 1:5,000), tubulin (Cell Signaling, 1:10,000), calnexin (Assay Design, 1:10,000), p-eIF2a (Cell Signaling, 1:2000), eIF2a (Cell Signaling, 1:2,000), ERP57 (Assay Design, 1:2,000), PDI (Assay Design, 1:5,000), HRD1 (Novus Biologicals, 1:1,000), ERO1L (Novus Biologicals, 1:2,000) and GRP78 (Santa Cruz, 1:1,000).

Statistical Analysis—Differences between compared groups were evaluated by performing two-tailed Student's *t* test, and $p < 0.05$ is considered significant.

RESULTS

Hemizygosity of Sel1l Predisposes Mice to HFD-induced Hyperglycemia—We recently reported that mice homozygous for a gene trap mutation in *Sel1l* (*Sel1l*$^{-/-}$) develop systemic ER stress and die during mid-gestation (35). To determine the functional role of SEL1L in adult pancreatic β-cells, we investigated whether haploid insufficiency of SEL1L affects glucose homeostasis in mice. Wild-type and *Sel1l*$^{+/-}$ male mice at 10 weeks of age were fed with normal chow (NC) and a high fat diet (HFD) for 20 weeks (Fig. 1*A*). *Sel1l*$^{+/-}$ and wild-type mice showed similar body weight gain profiles in response to the two diets (Fig. 1*B*). Basal fasting blood glucose levels of *Sel1l*$^{+/-}$ and wild-type mice were comparable (supplemental Fig. S1*A*) and remained insignificantly changed in response to NC feeding (Fig. 1*C*). However, after 8 weeks of HFD, *Sel1l*$^{+/-}$ mice showed significantly higher blood glucose levels than the wild-type control mice (Fig. 1*B*). These results indicate that mice with one functional allele of *Sel1l* are genetically predisposed to HFD-induced hyperglycemia.

Hyperglycemia in mice may be the result of a defective insulin production, action, or both. To determine the specific causes underlying the impaired glucose homeostasis in Sel1l$^{+/-}$ mice, we first assessed whether haploid insufficiency of SEL1L reduces insulin sensitivity in organs such as liver, skeletal muscle, and adipose tissue. Insulin tolerance tests showed that *Sel1l*$^{+/-}$ mice showed comparable insulin sensitivity to wild-type mice (Fig. 1*D*), suggesting that haploinsufficiency of SEL1L did not significantly affect peripheral insulin signaling. Next, we examined whether *Sel1l*$^{+/-}$ mice had an impaired β-cell function using glucose tolerance tests. *Sel1l*$^{+/-}$ and wild-type mice fed with NC showed similar glucose tolerance to wild-type control mice (supplemental Fig. S1*B*). However, *Sel1l*$^{+/-}$ mice fed with HFD exhibited significantly higher glucose intolerance than wild-type control mice (Fig. 1*E*). Administration of 4-PBA, a chemical chaperone previously shown to enhance insulin signaling (38), resulted in a significant reduction of serum glucose levels in both *Sel1l*$^{+/-}$ and wild-type mice fed with HFD (Fig. 1*F*). Together, these data suggest that in our current diet-induced obesity model, haploid insufficiency of *Sel1l* impairs insulin production in pancreatic β-cells and had little effect on insulin action in peripheral organs.

Haploid Insufficiency of SEL1L Impairs Glucose-stimulated Insulin Secretion and Adaptive Proliferation of β-Cells—We next assessed the serum insulin levels in *Sel1l*$^{+/-}$ mice fed with NC and HFD using insulin ELISA. No significant difference in serum insulin level was observed between *Sel1l*$^{+/-}$ and wild-type mice fed with NC. However, *Sel1l*$^{+/-}$ mice fed with HFD showed significantly higher serum insulin levels than wild-type control mice (Fig. 2*A*). The pancreatic insulin contents of wild-type and *Sel1l*$^{+/-}$ mice fed with HFD were comparable (supplemental Fig. S2*A*). We next carried out glucose-stimulated insulin secretion studies in *Sel1l*$^{+/-}$ mice. Although *Sel1l*$^{+/-}$ mice fed with NC showed no difference in GSIS to wild-type control mice (Fig. 2*C*), *Sel1l*$^{+/-}$ mice fed with HFD showed a significantly lower GSIS as compared with wild-type mice (Fig. 2*B*). These results together with the finding that *Sel1l*$^{+/-}$ mice were glucose-intolerant (Fig. 1*E*) indicate that haploid insufficiency of SEL1L also causes impairment in glucose-stimulated insulin secretion.

The functional β-cell mass is a critical factor in determining how much insulin is released into the blood in response to glucose stimulation. As *Sel1l*$^{+/-}$ mice showed an impaired pancreatic function, we speculated that *Sel1l*$^{+/-}$ mice fed with HFD might have a reduced β-cell mass. To test this, we carried out morphological analysis of the endocrine pancreas in *Sel1l*$^{+/-}$ fed with HFD. Wild-type and *Sel1l*$^{+/-}$ mice on HFD for 8 weeks showed no difference in β-cell masses (Fig. 2*C*). However, after 20 weeks of HFD-feeding, *Sel1l*$^{+/-}$ mice exhibited a markedly reduced β-cell mass as compared with that of wild-type mice (Fig. 2, *D–F*). We then investigated whether the reduction of β-cell mass in *Sel1l*$^{+/-}$ mice was due to an increased apoptosis or a decreased β-cell proliferation. *In situ* cell apoptosis assays showed that there was no significant difference in β-cell apoptosis between *Sel1l*$^{+/-}$ and wild-type

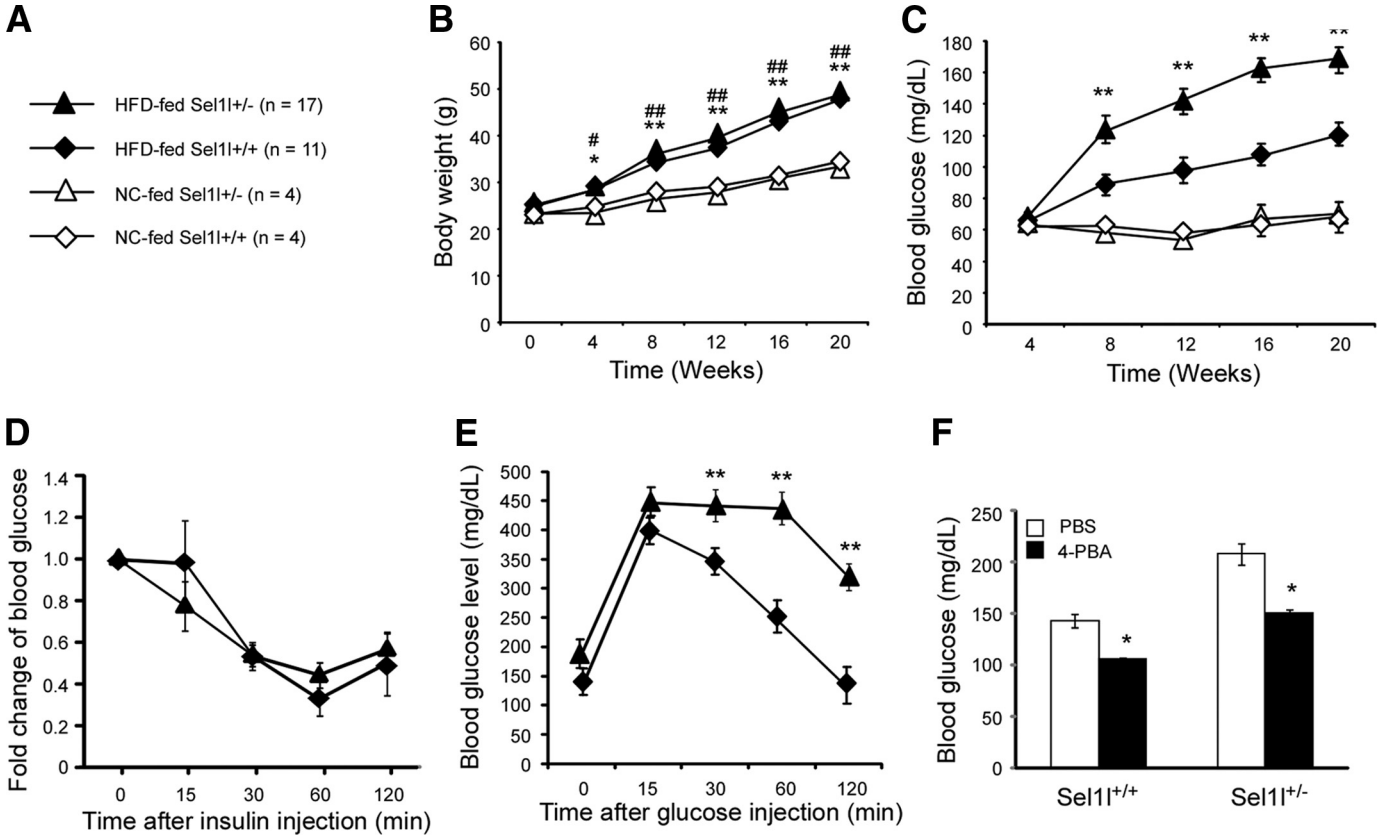

FIGURE 1. ***Sel1l*$^{+/-}$ mice are susceptible to HFD-induced hyperglycemia.** *A*, shown is a schematic representation of mouse groups and diets. 10-Week-old male *Sel1l*$^{+/-}$ and *Sel1l*$^{+/+}$ mice were randomly divided and fed with NC or a HFD, respectively, for 20 weeks. *B*, shown are body weight gains of *Sel1l*$^{+/-}$ and *Sel1l*$^{+/+}$ mice on a HFD or NC. *, $p < 0.05$; **, $p < 0.01$, *Sel1l*$^{+/-}$ HFD *versus* NC; #, $p < 0.05$; ##, $p < 0.01$, *Sel1l*$^{+/+}$ HFD *versus* *Sel1l*$^{+/+}$ NC. *C*, shown are fasting blood glucose levels of *Sel1l*$^{+/-}$ and *Sel1l*$^{+/+}$ mice on HFD or NC. **, $p < 0.01$, *Sel1l*$^{+/-}$ HFD *versus* *Sel1l*$^{+/+}$ HFD. *D*, shown is insulin tolerance of *Sel1l*$^{+/-}$ and *Sel1l*$^{+/+}$ mice fed with HFD for 24 weeks. *E*, shown is glucose tolerance of *Sel1l*$^{+/-}$ and *Sel1l*$^{+/+}$ mice on HFD for 20 weeks. **, $p < 0.01$, *Sel1l*$^{+/-}$ HFD ($n = 10$) *versus* *Sel1l*$^{+/+}$ HFD ($n = 11$). *F*, shown are fasting blood glucose levels of *Sel1l*$^{+/-}$ and *Sel1l*$^{+/+}$ mice on HFD for 20 weeks and treated with either PBS or 4-PBA for 1 week; *, $p < 0.05$ 4-PBA *versus* PBS ($n = 5$ per genotype). All values are expressed as the mean ± S.E.

mice (supplemental Fig. S2*B*). However, *Sel1l*$^{+/-}$ islets contained a significantly lower number of Ki67-positive β-cells than wild-type islets (Fig. 2, *G–I*). Together, these results indicate that *Sel1l*$^{+/-}$ mice fed with HFD for 20 weeks had a reduced β-cell mass, and the reduction of β-cell mass in *Sel1l*$^{+/-}$ mice was due at least in part to an impaired compensatory β-cell growth.

Haploinsufficiency of SEL1L Predisposes Liver and Pancreatic Islets to Obesity-induced Endoplasmic Reticulum Stress—SEL1L is a critical component of the ER-associated protein degradation machinery, and SEL1L deficiency results in systemic ER stress in mouse embryonic cells (35). We, therefore, next investigated possible alterations of the UPR pathway in liver and pancreatic islets of *Sel1l*$^{+/-}$ mice fed with HFD. First, we cultured islets isolated from wild-type and *Sel1l*$^{+/-}$ mice in the presence of low (10 mM) and high (30 mM) glucose and performed quantitative RT-PCR analysis of UPR marker genes. Wild-type and *Sel1l*$^{+/-}$ islets treated with low glucose showed comparable expression of *Bip*, *Herp*, *Chop*, *Xbp-1s*, and *p58IPK* at the mRNA level (Fig. 3*A*). However, *Bip*, *Herp*, *Chop*, and *Xbp-1s* were significantly up-regulated in high glucose-treated *Sel1l*$^{+/-}$ islets as opposed to wild-type control islets (Fig. 3*B*). Treatment of *Sel1l*$^{+/-}$ pancreatic islets with 30 mM glucose in the presence of the chemical chaperon 4-PBA markedly reduced the transcription of *Bip*, *Herp*, *Xbp-1s*, and *p58IPK* (Fig. 3*C*).

ER stress has previously been mechanistically linked to obesity-induced insulin resistance in mice (25). Because *Sel1l*$^{+/-}$ mice were modestly insulin-intolerant (Fig. 1*D*), we speculated that this might be due to low levels of ER stress in peripheral organs such as liver and adipose tissue. To test this, we prepared lysates from livers of *Sel1l*$^{+/-}$ and wild-type control mice fed with HFD and examined the expression of a number of UPR genes through Western blot analyses (Fig. 3*D*). The liver of *Sel1l*$^{+/-}$ mice showed significantly elevated expression of CALNEXIN, elF2a, ERP57, and BIP as compared with the liver of wild-type mice fed with the same diet (Fig. 3*E*). Quantitative RT-PCR also revealed significantly elevated expression of Chop and Ero1l mRNA (supplemental Fig. S3). These results indicate that haploinsufficiency of SEL1L predisposes liver and pancreatic islets to ER stress induced by obesity.

Interference of SEL1L Function in Vitro Markedly Inhibits Glucose-stimulated Insulin Secretion and β-Cell Proliferation—To further understand the role of SEL1L in regulating β-cell function and growth, we performed functional studies of SEL1L in insulinoma cell lines, Min6 and INS-1. First, we assessed the effect of ectopic expression of dSEL1L-GFP, a GFP-tagged SEL1L deletion mutant, on the secretion of G-luc, a naturally

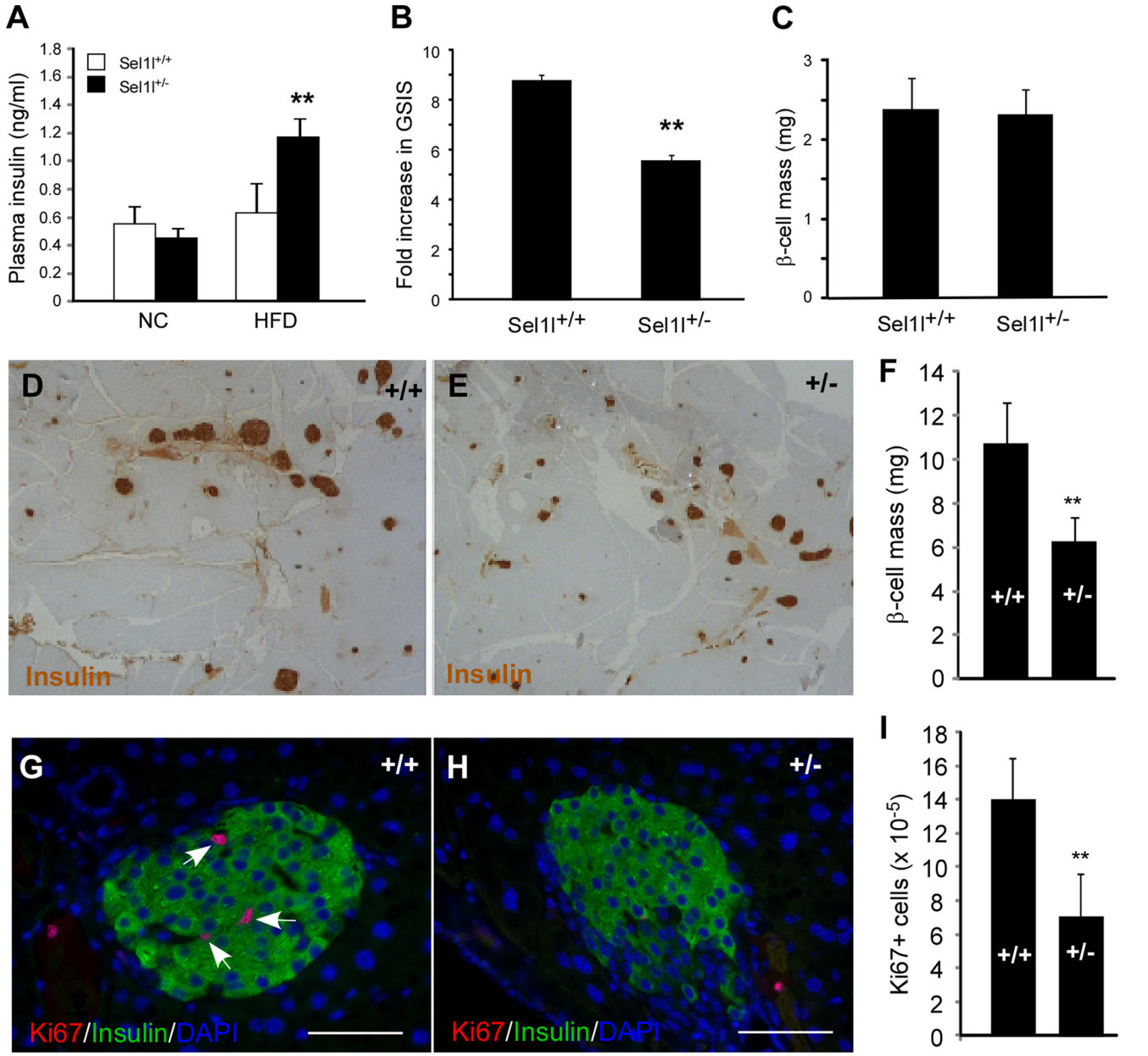

FIGURE 2. ***Sel1l*$^{+/-}$ mice fed with a high fat diet exhibit impaired GSIS and reduced β-cell mass.** *A*, shown are plasma insulin levels of *Sel1l*$^{+/-}$ and *Sel1l*$^{+/+}$ mice on NC or HFD for 20 weeks. **, $p < 0.01$ HFD-fed *Sel1l*$^{+/-}$ *versus* *Sel1l*$^{+/+}$ mice ($n = 7$). *B*, shown is fold change of GSIS of *Sel1l*$^{+/-}$ and *Sel1l*$^{+/+}$ mice. **, $p < 0.01$, *Sel1l*$^{+/-}$ *versus* *Sel1l*$^{+/+}$ mice ($n = 5$ per genotype). *C*, shown are β-cell masses of *Sel1l*$^{+/-}$ and *Sel1l*$^{+/+}$ mice on HFD for 8 weeks ($n = 7$ per genotype). *D–E*, shown are representative images of insulin immunostained pancreatic sections from *Sel1l*$^{+/+}$ (*D*) and *Sel1l*$^{+/-}$ (*E*) mice on HFD for 20 weeks. *F*, shown is quantification of β-cell mass in *Sel1l*$^{+/+}$ and *Sel1l*$^{+/-}$ mice on HFD for 20 weeks. **, $p < 0.01$ *Sel1l*$^{+/+}$ *versus* *Sel1l*$^{+/-}$ mice ($n = 5$ per genotype). β-Cell mass was determined by timing the pancreatic weight with percentage of the β-cell area. *G* and *H*, representative images are shown of Ki67 immunofluorescence of pancreatic sections from *Sel1l*$^{+/+}$ (*G*) and *Sel1l*$^{+/-}$ (*H*) mice on HFD for 20 weeks. Nuclei were countered stained with DAPI. *I*, shown is quantification of Ki67-positive cells in *Sel1l*$^{+/+}$ and *Sel1l*$^{+/-}$ mice on HFD for 20 weeks. The rate of β-cell proliferation was calculated by dividing the number of Ki67-positive cells with the total number of nuclei counted. **, $p < 0.01$ *Sel1l*$^{+/+}$ *versus* *Sel1l*$^{+/-}$ mice ($n = 4$ per genotype). All values are expressed as the mean ± S.E.

secreted luciferase reporter (46). G-luc and dSEL1L-GFP were transiently expressed in Min6 cells. Conditioned media of Min6 cells were collected at various time points after transfection and analyzed by luciferase assays. G-luc activities in the conditioned media of dSEL1L-GFP-expressing cells were significantly lower than those in the conditioned medium of GFP-expressing control cells (Fig. 4*A*). We then asked whether overexpression of SEL1L facilitates or enhances the secretion of G-luc. For this study we co-expressed SEL1L-GFP with a NHK-GFP, GFP-tagged null-Hong-Kong variant mutant human α1-antitrypsin in Min6 cells. NHK-GFP, an inherent folding-incompetent protein, was previously shown to induce ER stress in mammalian cells (47). Co-expression of SEL1L-GFP with NHK-GFP significantly increased the G-luc activity of conditioned media (Fig. 4*B*).

Although the luciferase data described above indicate that SEL1L function is critically required for general protein secretion in Min6 cells, we do not know if it is required for glucose-stimulated insulin secretion. Thus, we next examined whether ectopic expression of dSEL1L-GFP suppresses glucose-stimu-

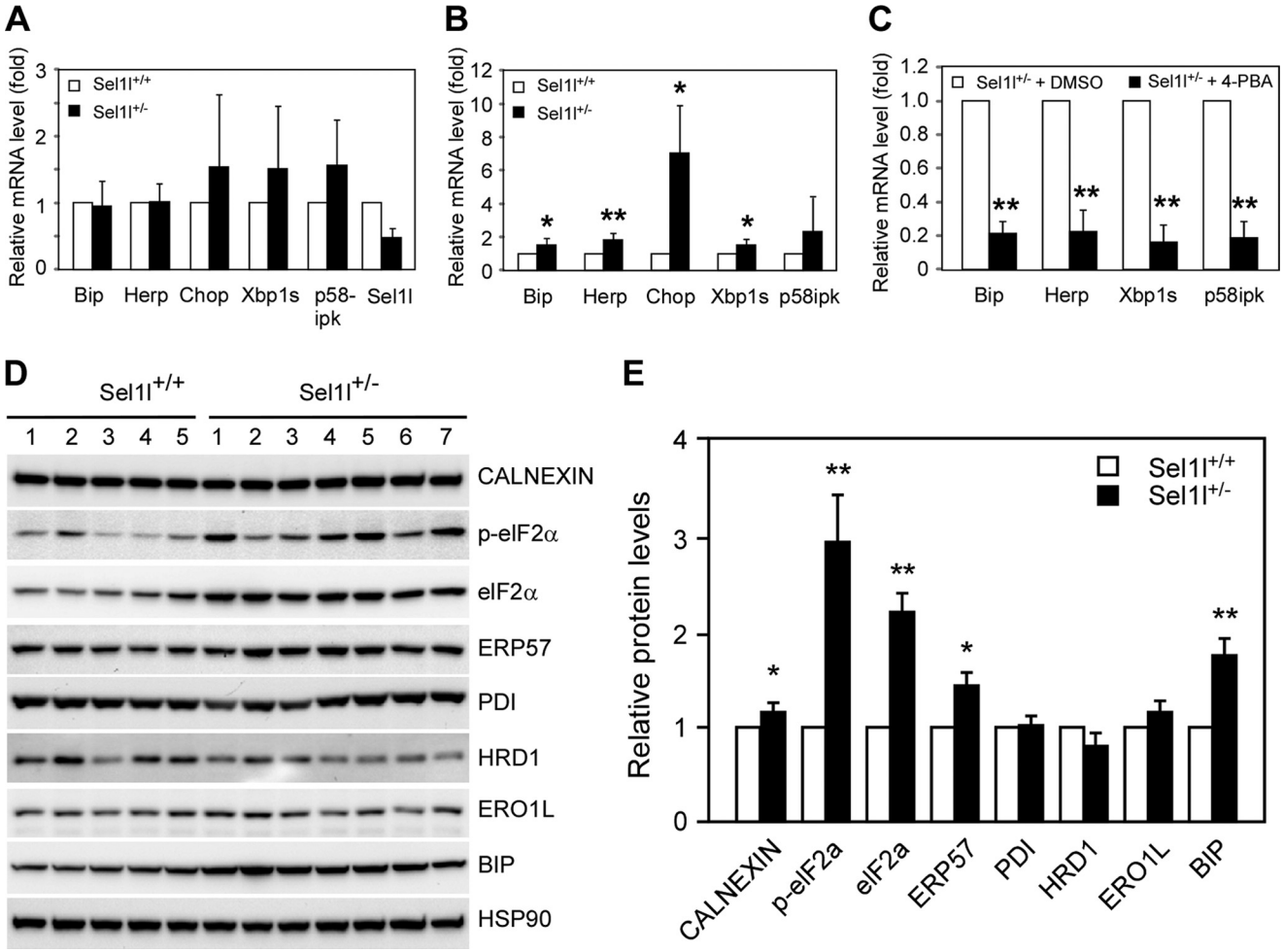

FIGURE 3. **Endoplasmic reticulum stress in pancreatic islets and liver of *Sel1l*$^{+/-}$ mice fed with a high fat diet.** *A* and *B*, shown is a comparison of UPR gene expression in *Sel1l*$^{+/+}$ and *Sel1l*$^{+/-}$ pancreatic islets. Islets were isolated from 30-week-old *Sel1l*$^{+/+}$ and *Sel1l*$^{+/-}$ mice and cultured overnight in media containing 10 mM (*A*) or 30 mM (*B*) glucose. The mRNA expression of five UPR genes, including Bip, Herp, Chop, Xbp1s, and p58IPK, were analyzed by real-time RT-PCR. *C*, real-time PCR analysis of UPR gene expression in *Sel1l*$^{+/-}$ islets treated with and without the chemical chaperon, 4-PBA is shown. For each gene, the expression in the vehicle (DMSO) treated islets was set to 1 and used to calculate a relative expression of the gene in 4-PBA treated islets. *D*, shown is UPR gene expression at the protein level in livers of *Sel1l*$^{+/-}$ and *Sel1l*$^{+/+}$ mice on HFD for 20 weeks. Liver lysates from 5 *Sel1l*$^{+/+}$ and 7 *Sel1l*$^{+/-}$ mice (30 μg per sample) were immunoblotted and probed with antibodies against the indicated gene products. HSP90 was used as a loading control. *E*, shown is quantification of protein expression in *Sel1l*$^{+/+}$ and *Sel1l*$^{+/-}$ mice indicated in *D*. For each protein the expression in *Sel1l*$^{+/+}$ liver was set to 1 and used to calculate a relative expression in *Sel1l*$^{+/-}$ liver. *, $p < 0.05$, **, $p < 0.01$ *Sel1l*$^{+/-}$ mice ($n = 7$) *versus* *Sel1l*$^{+/+}$ ($n = 5$). All values are expressed as the mean ± S.E.

lated insulin secretion in Min6 cells. For this study we generated stable Min6 cell lines containing a doxycycline-inducible dSel1l-GFP transgene. Doxycycline-dependent dSEL1L-GFP expression was verified by Western blot analysis (Fig. 4*C*). An insulin ELISA assay indicated that ectopic expression of dSEL1L-GFP in Min6 cells significantly reduced glucose-stimulated insulin secretion in Min6 cells (Fig. 4*D*).

Last, using the dominant-negative functional interference strategy detailed above, we assessed whether SEL1L function is critical for β-cell proliferation *in vitro*. For this study we generated INS-1 cell lines stably expressing the rtTA regulatory proteins (vehicle), rtTA + dSEL1L-GFP, and rtTA + SEL1L-GFP (Fig. 4*E*). Immunoblotting analysis showed that a significant up-regulation of Grp78/BIP expression was detectable at ~12 h after the activation of the dSel1l-GFP transgene in INS-1 cells (Fig. 4*F*). INS-1 lines stably expressing dSEL1L-GFP exhibited a significantly reduced cell proliferation as compared with control lines, as revealed by both cell number counting (Fig. 4*G*) and thymidine incorporation assays (Fig. 4*H*). Together, these results indicate that interference of SEL1L function in β-cells impairs both function (insulin secretion) and proliferation of β-cells.

DISCUSSION

The molecular mechanisms underlying the dysfunction and/or failure of β-cells in type 2 diabetes are the subject of many studies in recent years. Genetic studies in mice have implicated several ER proteins, including PERK, eIF2a, p58IPK, and WSF, in regulation of pancreatic β-cell growth and function. PERK-deficient mice became progressively diabetic during the postnatal period (48). p58IPK-deficient mice also gradually developed diabetes mellitus with increasing apoptosis of pancreatic islet cells (49). Mice homozygous null for *Wfs1* developed overt diabetes (50–52). In this study we provide genetic evidence that SEL1L is critically required for both β-cell function and proliferation. We show that mice heterozygous for a gene trap mutation in *Sel1l* (*Sel1l*$^{+/-}$) maintain normal glycemia under regular diet. However, when fed with a high fat

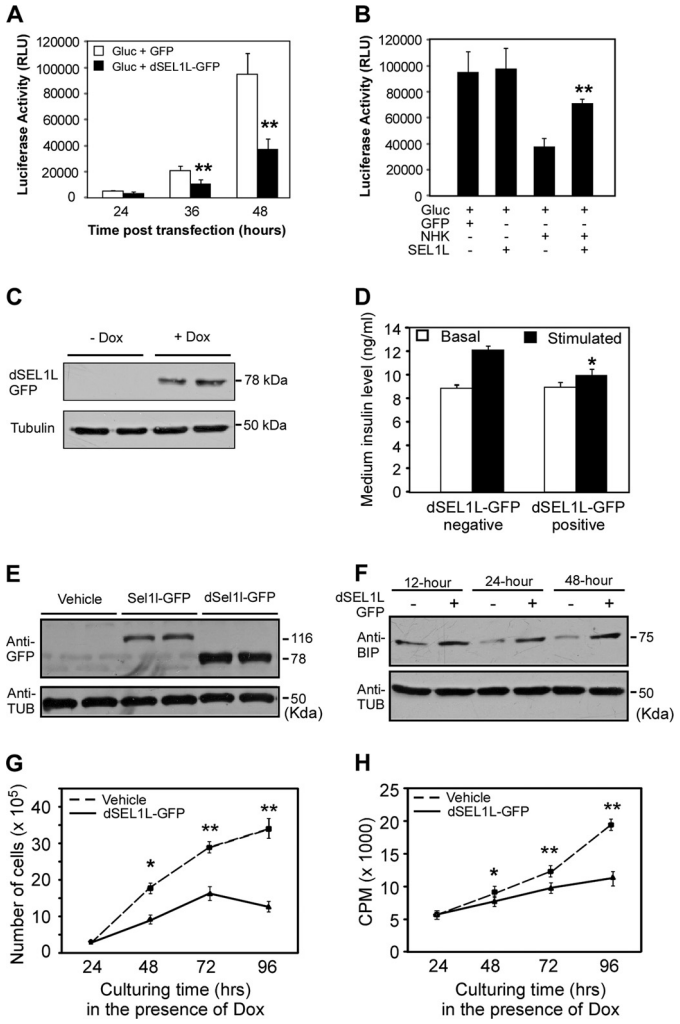

FIGURE 4. **Perturbation of SEL1L function in insulinoma cell lines impairs glucose-stimulated insulin secretion and β-cell proliferation.** *A*, G-luc secretion in Min6 cells transiently expressing a dominant-negative form of SEL1L is shown. Mins6 cells were transiently co-transfected with the indicated expression plasmids. Conditioned media were sampled at 24, 36, and 48 h post-transfection and analyzed by luciferase assay. Expression of dSel1l-GFP markedly suppresses G-luc secretion in Min6 cells. *B*, G-luc secretion in Min6 cells overexpressing SEL1L. Min6 cells were transiently co-transfected with the indicated expression plasmids. Conditioned media were sampled at 24 h post-transfection and analyzed by luciferase assay. Expression of SEL1L-GFP restores protein secretion inhibited by NHK-GFP. **, $p < 0.01$. NHK-GFP + SEL1L-GFP *versus* NHK-GFP- expressing cells. *C*, shown is an immunoblotting analysis of dSEL1L-GFP fusion protein expression in Min6 cells stably integrated with a Tet-inducible Sel1l-GFP transgene. dSEL1L-GFP was detected using an anti-GFP antibody. *Dox*, doxycycline. *D*, GSIS of Min6 cells stably expressing dSEL1L-GFP is shown. *, $p < 0.05$ dSEL1L-GFP-negative *versus* dSEL1L-GFP-positive cells. Expression of dSEL1L-GFP markedly inhibits glucose-stimulated insulin secretion in Min6 cells. *E*, shown is an immunoblotting analysis of SEL1L-GFP and dSEL1L-GFP expression in INS-1 cells stably integrated with Tet-inducible Sel1l-GFP and dSel1l-GFP transgenes. *F*, shown is an immunoblotting analysis of GRP78/BIP expression in INS-1 cells stably expressing dSEL1L-GFP. Ectopic expression of dSEL1L-GFP in INS-1 cells results in up-regulation of GRP78/BIP. *Tub*, tubulin *G* and *H*, shown are growth profiles of INS-1 cells stably expressing dSEL1L-GFP. Cell proliferation was analyzed through cell counting (*G*) and by thymidine incorporation assay (*H*). The data were derived from three independent experiments. *, $p < 0.05$; **, $p < 0.01$, vehicle *versus* dSEL1L-GFP expressing cells. All values are expressed as the mean ± S.E.

diet, *Sel1l*$^{+/-}$ mice exhibit a significantly elevated level of serum glucose. *Sel1l*$^{+/-}$ mice are glucose intolerant as compared with wild-type littermate controls. In addition, *Sel1l*$^{+/-}$ mice exhibit a markedly reduced β-cell mass due to a decreased rate of β-cell proliferation. Pancreatic islets from *Sel1l*$^{+/-}$ mice, when incubated *in vitro* in the presence of high glucose, exhibit an elevated expression of UPR genes. Furthermore, mouse and rat insulinoma cells stably expressing a dominant-negative form of SEL1L exhibit impaired protein secretion and cell growth. Together, these data strongly suggest that haploid insufficiency of SEL1L predisposes mice to high fat-induced hyperglycemia. Our findings thus support the hypothesis that SEL1L is a key regulator of glucose homeostasis in mice.

The pancreatic defects in *Sel1l*$^{+/-}$ mice are likely to be multifaceted and develop progressively during high fat diet feeding. *Sel1l*$^{+/-}$ mice exhibited significantly higher blood glucose levels than their wild-type littermates just after 8 weeks of HFD feeding (Fig. 1*C*). At this stage, however, no significant difference in β-cell mass was detected between *Sel1l*$^{+/-}$ and wild-type mice (Fig. 2*C*). These results argue that, at least initially, impaired glucose-stimulated insulin secretion was responsible for the observed dysregulated blood glucose homeostasis in *Sel1l*$^{+/-}$ mice on HFD. During further HFD feeding, the proliferation of pancreatic β-cells was inhibited (Fig. 2, *G–I*), leading to a significantly reduced β-cell mass (Fig. 2, *D–F*). Thus, the pancreatic defects at later phases of the HFD feeding are likely to be a combination of impaired insulin secretion and reduced β-cell mass.

Sel1l encodes an ER membrane protein that is highly expressed in the developing and mature pancreas (27). We previously demonstrated that SEL1L deficiency disrupts ER homeostasis, which leads to ER stress and activation of the unfolded protein response pathway (35). Several lines of evidence from the present study suggest that ER stress is likely to be responsible for the impaired insulin secretion and reduced β-cell proliferation in *Sel1l*$^{+/-}$ mice fed with HFD. First, we showed that *Sel1l*$^{+/-}$ islets treated with high glucose expresses significantly higher levels of UPR markers (Fig. 3*B*). Second, treatment of *Sel1l*$^{+/-}$ islets with the chemical chaperone, 4-PBA, markedly reduces the expression UPR genes. Third, INS-1 cells expressing a dominant-negative form of SEL1L exhibit significantly elevated expression of the ER stress sensors BIP. Further studies are required to elucidate how ER stress mechanistically affects β-cell growth and insulin secretion in adult mice.

The insulin signaling pathway in *Sel1l*$^{+/-}$ mice fed with HFD may also be impaired, as *Sel1l*$^{+/-}$ mice showed a significantly elevated plasma insulin level at the starting period of HFD feeding (Fig. 2*A*). The molecular mechanisms underlining the impaired insulin signaling in *Sel1l*$^{+/-}$ mice, however, remain unclear from the current investigation. SEL1L was previously shown to be a critical factor involved in regulating ER homeostasis (32, 33, 35). We show here that several factors of the unfolded protein response pathway are up-regulated in the liver of HFD-fed *Sel1l*$^{+/-}$ mice. It is thus conceivable that ER stress may be a contributing factor to the impaired insulin action in *Sel1l*$^{+/-}$ mice. This hypothesis is supported by the observation that treatment of HFD-fed *Sel1l*$^{+/-}$ mice with 4-PBA markedly lowers blood glucose levels (Fig. 1*F*). Proof of this requires further biochemical and molecular analyses of the liver and adipose tissues of *Sel1l*$^{+/-}$ mice on HFD.

The islet in type 2 diabetes is characterized by islet amyloid derived from islet amyloid polypeptide (53). Transgenic expression of human islet amyloid polypeptide in rodents recapitulates

this islet pathology and leads to diabetes (23, 54). Collectively, these findings suggest that islet amyloid plays an important role in mediating β-cell dysfunction and death. How amyloidogenesis occurs in islets of type 2 diabetes remains to be elucidated. However, given the role of SEL1L in quality control of ER-sorted proteins (32), it is tempting to speculate that dysregulation of SEL1L may be an underlying etiology for islet amyloidogenesis.

In conclusion, we show here that mice haploinsufficient for SEL1L are susceptible to HFD diet-induced hyperglycemia. These mice have a significantly reduced β-cell mass and an impaired glucose-stimulated insulin secretion. Our findings highlight a critical and previously unknown role for SEL1L in regulating β-cell function and growth. The implication of these findings is that SEL1L may have potential as a therapeutic target to develop new drugs for the prevention and treatment of type 2 diabetes mellitus.

Acknowledgments—We thank Dr. Donald F. Steiner (University of Chicago) for providing Min6 cells and Drs. Masakazu Shiota (Vanderbilt University) and Bruce Currie and Yves Boisclair (Cornell University) for stimulating discussions and critical comments during the preparation of this manuscript.

REFERENCES

1. American Diabetes Association (2008) *Diabetes Care* **31,** 596–615
2. Butler, A. E., Janson, J., Bonner-Weir, S., Ritzel, R., Rizza, R. A., and Butler, P. C. (2003) *Diabetes* **52,** 102–110
3. Carey, D. G., Jenkins, A. B., Campbell, L. V., Freund, J., and Chisholm, D. J. (1996) *Diabetes* **45,** 633–638
4. DeFronzo, R. A., Bonadonna, R. C., and Ferrannini, E. (1992) *Diabetes Care* **15,** 318–368
5. Eizirik, D. L., Cardozo, A. K., and Cnop, M. (2008) *Endocr. Rev.* **29,** 42–61
6. Scheuner, D., and Kaufman, R. J. (2008) *Endocr. Rev.* **29,** 317–333
7. Voeltz, G. K., Rolls, M. M., and Rapoport, T. A. (2002) *EMBO Rep.* **3,** 944–950
8. English, A. R., Zurek, N., and Voeltz, G. K. (2009) *Curr. Opin. Cell Biol.* **21,** 596–602
9. Hampton, R. Y. (2002) *Curr. Opin. Cell Biol.* **14,** 476–482
10. Ma, Y., and Hendershot, L. M. (2001) *Cell* **107,** 827–830
11. Sundar Rajan, S., Srinivasan, V., Balasubramanyam, M., and Tatu, U. (2007) *Indian J. Med. Res.* **125,** 411–424
12. Ron, D., and Walter, P. (2007) *Nat. Rev. Mol. Cell Biol.* **8,** 519–529
13. Harding, H. P., Novoa, I., Bertolotti, A., Zeng, H., Zhang, Y., Urano, F., Jousse, C., and Ron, D. (2001) *Cold Spring Harbor Symp. Quant. Biol.* **66,** 499–508
14. Brodsky, J. L. (2007) *Biochem. J.* **404,** 353–363
15. Ortsäter, H., and Sjöholm, A. (2007) *Mol. Cell. Endocrinol.* **277,** 1–5
16. van Anken, E., and Braakman, I. (2005) *Crit. Rev. Biochem. Mol. Biol.* **40,** 269–283
17. Straub, S. G., and Sharp, G. W. (2002) *Diabetes Metab. Res. Rev* **18,** 451–463
18. Orci, L., Ravazzola, M., Amherdt, M., Madsen, O., Perrelet, A., Vassalli, J. D., and Anderson, R. G. (1986) *J. Cell Biol.* **103,** 2273–2281
19. Lipson, K. L., Fonseca, S. G., and Urano, F. (2006) *Curr. Mol. Med.* **6,** 71–77
20. Boden, G., Duan, X., Homko, C., Molina, E. J., Song, W., Perez, O., Cheung, P., and Merali, S. (2008) *Diabetes* **57,** 2438–2444
21. Huang, C. J., Lin, C. Y., Haataja, L., Gurlo, T., Butler, A. E., Rizza, R. A., and Butler, P. C. (2007) *Diabetes* **56,** 2016–2027
22. Laybutt, D. R., Preston, A. M., Akerfeldt, M. C., Kench, J. G., Busch, A. K., Biankin, A. V., and Biden, T. J. (2007) *Diabetologia* **50,** 752–763
23. Matveyenko, A. V., Gurlo, T., Daval, M., Butler, A. E., and Butler, P. C. (2009) *Diabetes* **58,** 906–916
24. Oyadomari, S., Koizumi, A., Takeda, K., Gotoh, T., Akira, S., Araki, E., and Mori, M. (2002) *J. Clin. Invest.* **109,** 525–532
25. Ozcan, U., Cao, Q., Yilmaz, E., Lee, A. H., Iwakoshi, N. N., Ozdelen, E., Tuncman, G., Görgün, C., Glimcher, L. H., and Hotamisligil, G. S. (2004) *Science* **306,** 457–461
26. Donoviel, D. B., Donoviel, M. S., Fan, E., Hadjantonakis, A., and Bernstein, A. (1998) *Mech. Dev.* **78,** 203–207
27. Biunno, I., Appierto, V., Cattaneo, M., Leone, B. E., Balzano, G., Socci, C., Saccone, S., Letizia, A., Della Valle, G., and Sgaramella, V. (1997) *Genomics* **46,** 284–286
28. Biunno, I., Cattaneo, M., Orlandi, R., Canton, C., Biagiotti, L., Ferrero, S., Barberis, M., Pupa, S. M., Scarpa, A., and Ménard, S. (2006) *J. Cell. Physiol.* **208,** 23–38
29. Cattaneo, M., Otsu, M., Fagioli, C., Martino, S., Lotti, L. V., Sitia, R., and Biunno, I. (2008) *J. Cell. Physiol.* **215,** 794–802
30. Cormier, J. H., Tamura, T., Sunryd, J. C., and Hebert, D. N. (2009) *Mol. Cell* **34,** 627–633
31. Hosokawa, N., Wada, I., Nagasawa, K., Moriyama, T., Okawa, K., and Nagata, K. (2008) *J. Biol. Chem.* **283,** 20914–20924
32. Mueller, B., Klemm, E. J., Spooner, E., Claessen, J. H., and Ploegh, H. L. (2008) *Proc. Natl. Acad. Sci. U.S.A.* **105,** 12325–12330
33. Mueller, B., Lilley, B. N., and Ploegh, H. L. (2006) *J. Cell Biol.* **175,** 261–270
34. Oresic, K., Mueller, B., and Tortorella, D. (2009) *Biosci. Rep.* **29,** 173–181
35. Francisco, A. B., Singh, R., Li, S., Vani, A. K., Yang, L., Munroe, R. J., Diaferia, G., Cardano, M., Biunno, I., Qi, L., Schimenti, J. C., and Long, Q. (2010) *J. Biol. Chem.* **285,** 13694–13703
36. Li, S., Francisco, A. B., Munroe, R. J., Schimenti, J. C., and Long, Q. (2010) *BMC Dev. Biol.* **10,** 19
37. Sachdeva, M. M., Claiborn, K. C., Khoo, C., Yang, J., Groff, D. N., Mirmira, R. G., and Stoffers, D. A. (2009) *Proc. Natl. Acad. Sci. U.S.A.* **106,** 19090–19095
38. Ozcan, U., Yilmaz, E., Ozcan, L., Furuhashi, M., Vaillancourt, E., Smith, R. O., Görgün, C. Z., and Hotamisligil, G. S. (2006) *Science* **313,** 1137–1140
39. Gupta, S., McGrath, B., and Cavener, D. R. (2010) *Diabetes* **59,** 1937–1947
40. Scharp, D. W., Kemp, C. B., Knight, M. J., Ballinger, W. F., and Lacy, P. E. (1973) *Transplantation* **16,** 686–689
41. Zhang, W., Feng, D., Li, Y., Iida, K., McGrath, B., and Cavener, D. R. (2006) *Cell Metab.* **4,** 491–497
42. Miyazaki, J., Araki, K., Yamato, E., Ikegami, H., Asano, T., Shibasaki, Y., Oka, Y., and Yamamura, K. (1990) *Endocrinology* **127,** 126–132
43. Dowling, P., O'Driscoll, L., O'Sullivan, F., Dowd, A., Henry, M., Jeppesen, P. B., Meleady, P., and Clynes, M. (2006) *Proteomics* **6,** 6578–6587
44. Merglen, A., Theander, S., Rubi, B., Chaffard, G., Wollheim, C. B., and Maechler, P. (2004) *Endocrinology* **145,** 667–678
45. Li, S., Francisco, A. B., Han, C., Pattabiraman, S., Foote, M. R., Giesy, S. L., Wang, C., Schimenti, J. C., Boisclair, Y. R., and Long, Q. (2010) *FEBS Lett.* **584,** 4121–4127
46. Badr, C. E., Hewett, J. W., Breakefield, X. O., and Tannous, B. A. (2007) *PLoS One* **2,** e571
47. Sifers, R. N., Brashears-Macatee, S., Kidd, V. J., Muensch, H., and Woo, S. L. (1988) *J. Biol. Chem.* **263,** 7330–7335
48. Harding, H. P., Zeng, H., Zhang, Y., Jungries, R., Chung, P., Plesken, H., Sabatini, D. D., and Ron, D. (2001) *Mol. Cell* **7,** 1153–1163
49. Ladiges, W. C., Knoblaugh, S. E., Morton, J. F., Korth, M. J., Sopher, B. L., Baskin, C. R., MacAuley, A., Goodman, A. G., LeBoeuf, R. C., and Katze, M. G. (2005) *Diabetes* **54,** 1074–1081
50. Akiyama, M., Hatanaka, M., Ohta, Y., Ueda, K., Yanai, A., Uehara, Y., Tanabe, K., Tsuru, M., Miyazaki, M., Saeki, S., Saito, T., Shinoda, K., Oka, Y., and Tanizawa, Y. (2009) *Diabetologia* **52,** 653–663
51. Ishihara, H., Takeda, S., Tamura, A., Takahashi, R., Yamaguchi, S., Takei, D., Yamada, T., Inoue, H., Soga, H., Katagiri, H., Tanizawa, Y., and Oka, Y. (2004) *Hum. Mol. Genet.* **13,** 1159–1170
52. Riggs, A. C., Bernal-Mizrachi, E., Ohsugi, M., Wasson, J., Fatrai, S., Welling, C., Murray, J., Schmidt, R. E., Herrera, P. L., and Permutt, M. A. (2005) *Diabetologia* **48,** 2313–2321
53. Butler, A. E., Janson, J., Soeller, W. C., and Butler, P. C. (2003) *Diabetes* **52,** 2304–2314
54. Janson, J., Soeller, W. C., Roche, P. C., Nelson, R. T., Torchia, A. J., Kreutter, D. K., and Butler, P. C. (1996) *Proc. Natl. Acad. Sci. U.S.A.* **93,** 7283–7288